to appear in Applied Physics B, Special Issue "Optical Properties of Nanoparticles" manuscript No.
(will be inserted by the editor)

Collectivity in the optical response of small metal clusters

S. Kümmel[1], **K. Andrae**[2], **P.-G. Reinhard**[2]

[1] Department of Physics and Quantum Theory Group, Tulane University, New Orleans, Louisiana 70118, USA
[2] Institut für Theoretische Physik, Universität Erlangen, D-91077 Erlangen, Germany

Received: / Revised version:

Abstract The question whether the linear absorption spectra of metal clusters can be interpreted as density oscillations (collective "plasmons") or can only be understood as transitions between distinct molecular states is still a matter of debate for clusters with only a few electrons. We calculate the photoabsorption spectra of Na_2 and Na_5^+ comparing two different methods: quantum fluid-dynamics and time-dependent density functional theory. The changes in the electronic structure associated with particular excitations are visualized in "snapshots" via transition densities. Our analysis shows that even for the smallest clusters, the observed excitations can be interpreted as intuitively understandable density oscillations. For Na_5^+, the importance of self-interaction corrections to the adiabatic local density approximation is demonstrated.

PACS: 36.40.Vz, 31.15.Ew

1 Introduction

Among the earliest experiments providing insight into the electronic structure of metal clusters were measurements of the linear photoabsorption spectra [1,2]. Today, still, they are among the most powerful probes of a cluster's structure, and understanding the effects of collectivity in absorption spectra in general is also one prerequisite for understanding the nonlinear regime that is being probed experimentally with increasing sophistication [3]. In particular for positively charged sodium clusters, linear spectra have been measured for a broad range of cluster sizes and temperatures [4]. Typically, the experiments show a few strong absorption lines that exhaust most of the oscillator strength. However, despite the fact that the absorption spectra have been known for a long time, their theoretical interpretation is still being discussed. Since sodium is the nearly-free electron metal par excellence, allowing to study metallic behavior in one of its purest forms, a lot of theoretical work over the years has been devoted to photoabsorption in Na clusters [5,6,7,8,9,10,11,12,13,14,15]. From these studies, two different and somewhat opposing points of view on the interpretation of the observed resonances emerged. On the one hand, small clusters can accurately be described in the language of quantum chemistry, understanding the excitations as transitions between distinct molecular (electronic) states. On the other hand, the experiments found an early, intuitive interpretation in terms of collective oscillations of the valence electron density against the inert ionic background, similar to the plasmon in bulk metals or the giant resonances in atomic nuclei. Since the strong delocalization of the valence electrons that characterizes nearly free electron metals is found even in the smallest Na clusters, it has been argued that the second interpretation should also be applicable to small clusters.

A theoretically well founded [16] and practically tested [5,9,10,12,13,15] method for the theoretical investigation of excitations in metal clusters is time dependent density functional theory (TDDFT) at the level of the adiabatic, time-dependent local density approximation (TDLDA). A refinement of TDLDA corrects for the self-interaction error leading to the scheme of a time-dependent self-interaction correction simplified by a global averaging procedure (TDSIC) [12]. A somewhat simpler, yet powerful, alternative is quantum fluid-dynamics. In an extension of earlier works [6,7], quantum fluid-dynamics in a local current approximation (LCA) was recently derived making direct use [17] of the ground-state energy functional of density functional theory. In this work we are comparing these methods using two very small clusters as test cases with a threefold aim: First, comparing LCA to TDDFT for exactly the same system allows to judge on the reliability of LCA results. Second, by comparing TDLDA to its on-average self-interaction corrected counterpart, we check the impact of self-interaction corrections on low-energy photoabsorption spectra. Third,

Correspondence to: skuemmel@tulane.edu

the combination of methods allows us to demonstrate that, indeed, the experimental spectra for even the smallest clusters can be interpreted as valence electron density oscillations, leading to an intuitive understanding of the experimentally observed effects.

In section 2 our theoretical methods are reviewed. Section 3 presents the results for Na_2 and Na_5^+, which are discussed and summarized in section 4.

2 Theory

Starting point of our investigations is the usual ground-state energy functional

$$E[n;\{\mathbf{R}\}] = T_{\rm s}[\{\varphi\}] + E_{\rm xc}[n] + \int n(\mathbf{r})\, V_{\rm ion}(\mathbf{r};\{\mathbf{R}\})\, {\rm d}^3r + \frac{e^2}{2}\int\int \frac{n(\mathbf{r})n(\mathbf{r}')}{|\mathbf{r}-\mathbf{r}'|}\, {\rm d}^3r'\, {\rm d}^3r + \frac{Z^2e^2}{2}\sum_{\substack{i,j=1\\ i\neq j}}^{N} \frac{1}{|\mathbf{R}_i-\mathbf{R}_j|} \qquad (1)$$

for a cluster of N ions of valence Z (for Na, $Z=1$), valence-electron density n and ionic coordinates $\{\mathbf{R}\}$. The noninteracting kinetic energy $T_{\rm s}$ is calculated from the Kohn-Sham orbitals $\{\varphi\}$ and $E_{\rm xc}[n]$ denotes the exchange and correlation energy for which we use the LDA functional of Ref. [18]. Generalized gradient approximations, e.g. [19], in general lead to a better description of correlation effects in small systems. However, in the present case LDA is not too bad an approximation due to the strong delocalization of the valence electrons. $V_{\rm ion}$ is the sum of pseudopotentials $V_{\rm ion}(\mathbf{r};\{\mathbf{R}\}) = \sum_{i=1}^{N} v_{\rm ps}(|\mathbf{r}-\mathbf{R}_i|)$. We employ the smooth-core pseudopotential of Ref. [14]. In combination with LDA it provides accurate bond lengths, which are important for optical absorption spectra and polarizabilities [14,20]. The ionic coordinates were obtained by self-consistent minimization of the functional (1) with respect to both n and $\{\mathbf{R}\}$ and are given in Ref. [14]. The Kohn-Sham equations are solved directly, i.e., without basis sets, on a real space grid. We have verified that the coordinates obtained in the symmetry restricted optimizations of Ref. [14] do not change noticeably if the optimization is done fully three-dimensional. In order to be consistent, the ionic configurations were reoptimized on the SIC level for the TDSIC calculations, as discussed below.

Eq. (1) is also the key ingredient for the quantum fluid-dynamical LCA. A detailed discussion of the theory can be found in Ref. [17]. Therefore, we here restrict ourselves to a brief sketch. The essential idea of LCA is to describe excitations as harmonic density oscillations. The oscillating density is obtained from the scaling transformation

$$n(\mathbf{r},\alpha(t)) = e^{-\alpha(t)S_n} n(\mathbf{r}), \qquad (2)$$

where $\alpha(t) \propto \cos\omega t$ and S_n is the so called density scaling operator

$$S_n = \Big(\nabla \mathbf{u}(\mathbf{r})\Big) + \mathbf{u}(\mathbf{r})\cdot\nabla, \qquad (3)$$

which contains – hallmark of a fluid-dynamical description – a displacement field $\mathbf{u}(\mathbf{r})$. A similar, consistent transformation is also applied to the Kohn-Sham orbitals from which the density is constructed. From a variational principle and Eq. (1), a set of coupled, partial differential eigenvalue equations for the Cartesian components of $\mathbf{u}$ is derived. The eigenvalues are the excitation energies, and from the solutions $\mathbf{u}_\nu$, absolute oscillator strengths and intrinsic current densities

$$\mathbf{j}_\nu(\mathbf{r},t) = \dot{\alpha}_\nu(t)\, \mathbf{u}_\nu(\mathbf{r})\, n_\nu(\mathbf{r},\alpha_\nu(t)) \qquad (4)$$

associated with a particular (the ν-th) excitation are derived. Eq. (4) is the reason for the name "local current approximation". If a mode $\mathbf{j}_\nu$ can be excited by the dipole operator $D=-ez$ we call it a z-mode (or x,y, respectively).

It is important to note that the LCA is not a (semi) classical but a quantum mechanical method in the sense that it is derived on the basis of the quantum mechanical Kohn-Sham energy functional, which contains information on the quantal single-particle states in the kinetic energy. But the range of validity for the LCA is hard to assess formally [21]. However, gathering experience on its performance, as done for earlier versions which were truly semiclassical methods [6] or approaches using a well guessed expansion basis of local operators [7], will lead to a better understanding. It is therefore one aim of the present work to test the accuracy of the LCA by comparing it to the well established TDLDA.

For TDLDA and TDSIC, the numerical solution of the Kohn-Sham equations is done on a spatial grid with Fourier transformation for the definition of the kinetic energy. Accelerated gradient iteration is used for the static part. The dynamic propagation is done with the time-splitting method. For details of the technology see the review [22]. The spectra are computed as described in [22,23,24]. We start from the electronic and ionic ground state configuration. An instantaneous boost of the whole electron density initializes the dynamical evolution according to time-dependent LDA or SIC. The emerging dipole momentum as function of time is finally Fourier transformed into the frequency domain. This delivers the spectral distribution of dipole strength. The initial boost is kept small enough for the method to produce the spectra in the regime of linear response.

3 Results

With the methods described in the previous section we first investigated the sodium dimer. At first glance, it could be expected that the two-electron system Na_2 is

Table 1 Dipole excitations up to 4 eV for Na_2. Energies EE in eV and oscillator strengths OS as percentages of the dipole sumrule $m_1 = e^2\hbar^2 NZ/(2m)$ for LCA (superscript a), TDLDA (superscript b) and TDSIC (superscript c). Columns labeled "mode" indicate the direction of oscillation, see text for discussion. For comparison, we also list TDLDA results (superscript d) and experimental values (superscript e) from Ref. [15]. — indicates that the corresponding mode is not found in LCA, - that the strength in TDSIC was beyond numerical accuracy, no v. that no corresponding value has been given in the literature.

EE^a	OS^a	$Mode^a$	EE^b	OS^b	$Mode^b$	EE^c	OS^c	EE^d	OS^d	EE^e
1.93	30.9	z	2.09	31	z	2.13	36	2.09	31.4	1.82
2.56	58.9	x/y	2.63	56	x/y	2.65	57	2.52	53.1	2.52
3.93	1.7	z	3.67	1	z	3.89	-	3.28	<1	3.64
—	—	—	3.72	3	x/y	3.95	-	no v.	no v.	no v.

not described accurately in the quantum fluid-dynamical LCA. However, as seen from Fig. 1, TDLDA and LCA give similar results. Since the LCA currents were calculated with the LDA functional, we first compare them to TDLDA and discuss TDSIC results later. It is important to note that our TDLDA and LCA calculations were performed on exactly the same basis, i.e, using the same internuclear distance and pseudopotential. For a closer inspection we give in Table 1 the excitation energies and percentages on the dipole sumrule for the excitations up to 4 eV that carry most of the oscillator strength. Comparing columns 1–3 to columns 4–6 reveals some noteworthy differences between LCA and TDLDA. First, for the lowest excitation, LCA gives an energy lower than TDLDA with a difference larger than the numerical uncertainty. Since LCA rests on a variational principle, the fact that it leads to a lower excitation energy than TDLDA points at that it can be seen as an independent method. In this context we also note that our TDLDA for the z-excitation is consistent with the result in [15]. Second, whereas LCA is very accurate for the two low-lying, strong transitions, it does not seem to perform as well for the higher lying excitations. For technical reasons, the oscillator strength for the weak transitions is hard to asses in our TDLDA and TDSIC and could only be estimated in TDLDA. However, Fig. 1 shows that in comparison to TDLDA, the strength of the third peak is underestimated in LCA, and the LCA eigenvalue is too high. Tab. 1 shows why the TDLDA spectrum in Fig. 1 looks better. Whereas LCA only leads to one z mode, TDLDA around 3.7 eV gives excitations in both z and x/y direction. A "double-peak" structure has also been found in other TDLDA calculations [13]. Thus, we conclude that LCA gives some of the strength carried by transitions at higher energies, but it does not provide the same resolution as TDLDA. This is understandable since TDLDA embraces the whole fragmentation into the various one-particle-hole ($1ph$) states of the excitation spectrum, while LCA is bound to a "collective deformation path".

For Na_2, TDSIC leads to overall similar results as TDLDA, therefore we do not show the spectrum in a separate plot. Besides the fact that the TDSIC spectrum does not show the "cut" in the low energy shoulder of

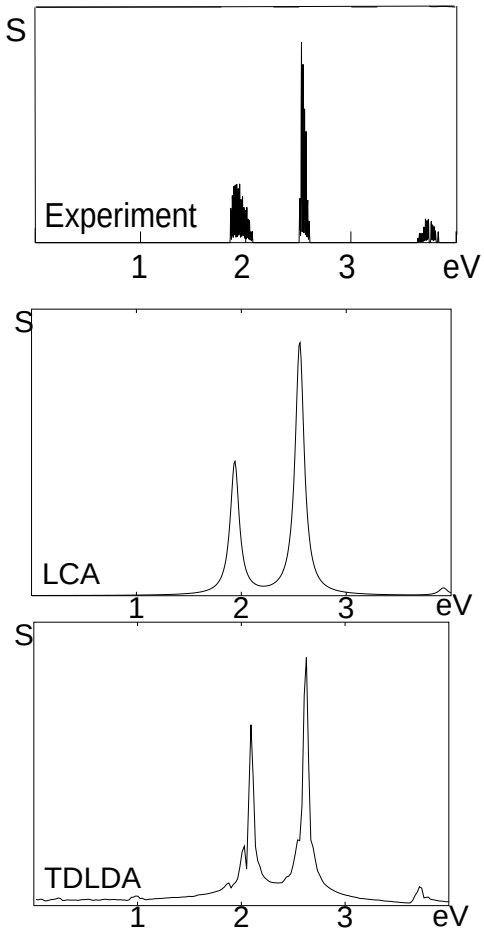

Fig. 1 Experimental [25], LCA and TDLDA photoabsorption spectrum S of Na_2 in arbitrary units against excitation energy in eV. The line broadening is chosen phenomenologically to match the experiment.

the excitation at 2.09 eV, the main difference is that TDSIC leads to slightly higher excitation energies than TDLDA (see Tab. 1). The deviation is less than 0.05 eV for the low-lying, strong transitions, but it is more than 0.2 eV for the higher ones (placing them at a similar energy as LCA). The reason is that the bonding distance is 0.1 a_0 smaller than in LDA [12]. This slight compression leads to a small blue shift. The higher excitations are

more sensitive because they are dominantly $1ph$ transitions, and it is known that SIC has stronger effects on the single-particle states. A recent, detailed discussion of how several other approximations for $E_{\rm xc}$ influence the dimer spectrum can be found in [15].

An intuitive understanding of the observed excitations can be obtained by looking at "snapshots of the density change". In LCA, these are easily accessible since the local currents, Eq. (4), obey the continuity equation

$$\nabla \mathbf{j}_\nu + \frac{\mathrm{d}n_\nu(\mathbf{r},t)}{\mathrm{d}t} = 0. \qquad (5)$$

Thus, one only needs to numerically calculate and then plot the divergence of $\mathbf{j}_\nu$ to obtain a visualization of the density change associated with the ν-th excitation at one particular instant. This can be done separately for each LCA eigenmode. As an analogon in TDLDA, we record the time evolution of the density $n(\mathbf{r},t)$ and evaluate the Fourier components

$$\tilde{n}(\mathbf{r},\omega_\nu) = \int n(\mathbf{r},t)\,\exp(-i\omega_\nu t)\mathrm{d}t \qquad (6)$$

for the frequencies ω_ν that are associated with particular excitations. Since this procedure is numerically more demanding, we have restricted the TDLDA analysis to a one dimensional section along the axis of symmetry, integrating (6) over x and y coordinates.

The top left picture in Fig. 2 shows a contour plot of the ground-state valence electron density of Na_2 in a plane containing the axis of symmetry. (The grid for the calculation was larger than the shown part.) The ionic cores are clearly visible since they repel the valence electrons, leading to "holes" in the density. The bottom left picture visualizes how this valence electron density changes in time at the first excitation. Dark colors indicate a density increase, light colors a decrease. Obviously, the electron density increases at one end of the molecule and decreases at the other end. Thus, the valence electrons are shifted predominantly along the axis of symmetry. But the shift is not a uniform, simple translation of the density along the dipole field (as it would be obtained from the sumrule estimate [26]), but the intrinsic structure of the cluster is impressed on and reflected in the currents, leading to a shift "around" the ionic cores. The second excitation in LCA is a (twofold degenerate) x/y mode. Its density change (not shown in Fig. 2) is predominantly perpendicular to the axis of symmetry, as one also naively would expect. The third LCA excitation, shown in the top right picture, is again a z mode. The regions of strongest density variation are shifted compared to the first z mode, and the oscillation pattern shows a node at greater separation from the ionic cores. This reflects the mathematical requirement of orthogonality for the different modes [6,17,27],

$$\int \mathbf{u}_\nu(\mathbf{r})\mathbf{u}_\mu(\mathbf{r})\,n(\mathbf{r})\,\mathrm{d}^3r \propto \delta_{\mu\nu}. \qquad (7)$$

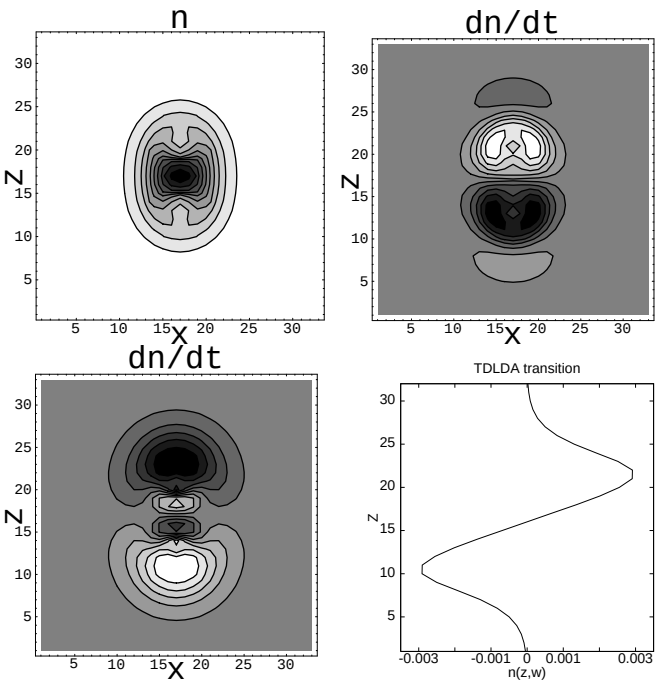

Fig. 2 "Snapshots" of the changes in valence electron density associated with particular excitations of Na_2. Contour plots show a plane containing the axis of symmetry of the molecule. Unit for the axes is the numerical grid spacing, 0.8 a_0. Top left: ground-state valence electron density n. Bottom left: $\mathrm{d}n/\mathrm{d}t$ associated with the first excitation, i.e. first z-mode, in LCA. Top right: $\mathrm{d}n/\mathrm{d}t$ associated with the third excitation, i.e. second z-mode, in LCA. Shadings lighter than the background gray indicate a density decrease, darker shadings an increase. Bottom right: $\tilde{n}(\mathbf{r},\omega_\nu)$ integrated over x and y as a function of z for lowest (i.e., $\nu = 1$) TDLDA excitation. The pictures are in accordance with understanding the excitations as density oscillations (see text).

Physically, the plots show that the observed electronic transitions can be interpreted as different eigenmodes, i.e., intrinsic oscillation patterns of the valence electron distribution. The TDLDA transition densities confirm this picture. The bottom right part of Fig. 2 shows Eq. (6) evaluated for the frequency of the lowest mode. Since x and y coordinate have been integrated over, some of the finer structure might have been smoothed out. But it is clearly visible that also in TDLDA, the lowest excitation is associated with a density increase at one end of the molecule and a decrease at the other. The regions of maximum density change are found very similar in LCA and TDLDA. We have verified this also for the second excitation that is not shown in Fig. 2. Thus, the simple picture of excitations as density oscillations seems to be remarkably close to the truth, even for the small Na_2.

Fig. 3 shows the experimental low-temperature photoabsorption spectrum [4] of Na_5^+ and below the spectra obtained in TDSIC, TDLDA, and LCA. Again, the LCA results (bottom) are shown with a phenomenological line broadening to make comparison with TDLDA easier. Overall, the spectrum obtained in LCA is rather

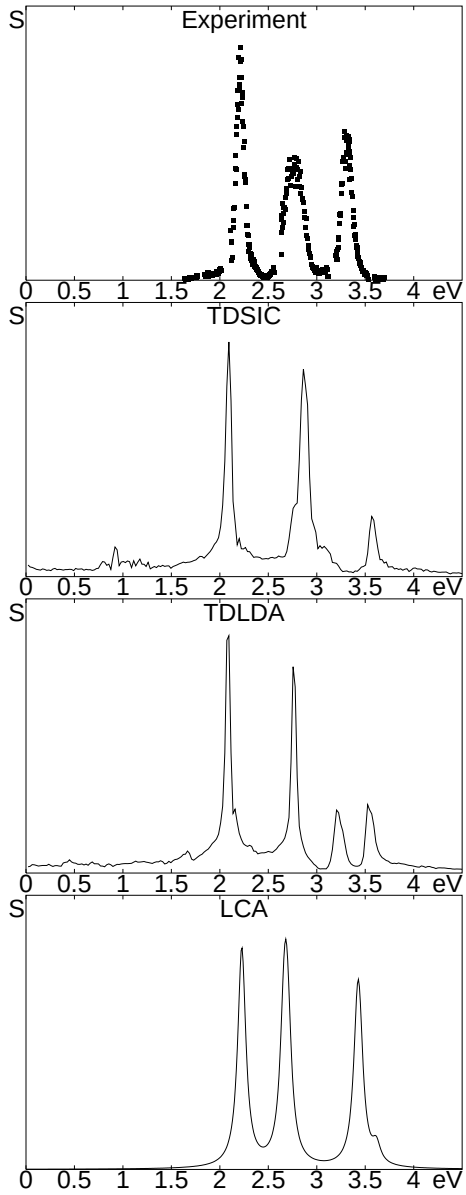

Fig. 3 From top to bottom: Experimental [4], TDSIC, TDLDA and LCA photoabsorption spectrum S of Na_5^+ in arbitrary units against excitation energy in eV.

close to the experiment, which again is remarkable in view of the small cluster size. However, our main focus here is on the comparison between TDLDA and TDSIC. TDLDA gives the energies and relative peak heights for the two lower transitions close to the experimental ones. But instead of one peak that is seen experimentally at about 3.3 eV, TDLDA leads to two peaks at 3.20 eV and 3.53 eV. A similar pattern was also found but not explained in recent TDLDA calculations [28] that focused on the explanation of the observed linewidths. By going over to TDSIC, we can further investigate the nature of the double peak. The TDSIC spectrum in Fig. 3 shows noticeable differences to TDLDA. First, a small subpeak is found at 0.92 eV. It is a relic of a $1ph$ excitation which originally was close to 1 eV and which has given most of its strength to the dominant peak. The comparable state in TDLDA is found at about 1.5 eV, i.e., so close to the main peak that its strength is hardly recognizable. Second, whereas the peak at 2.09 eV is hardly changed by the averaged SIC, the peak which in TDLDA was at 2.76 eV shifts to 2.86 eV in TDSIC and appears broader since there is another transition close by at 3.03 eV. This might contribute to explaining why also in the experimental low temperature data, the middle peak appears to be somewhat broader. Finally, the last excitation again stays nearly unchanged at 3.57 eV. Thus, by shifting the peak which in our TDLDA is found at 3.20 eV to lower energies, TDSIC leads to a spectrum that is close to the experimental one. We also tested whether this is only an indirect effect, due to slight rearrangements when the ionic geometry is re-optimized on SIC level. However, this is not the case: even when compared for exactly the same ionic structure, TDLDA and TDSIC spectra show noticeable differences. We find, in accordance with earlier investigations [12], that TDSIC leaves the main resonance peaks basically unchanged, but it strongly modifies the single-particle energies, and thus the underlying $1ph$ excitation spectrum. Our comparison with experimental data shows that while TDLDA gives reasonable results for the gross features of a spectrum, it can be inaccurate for details. In the energy range and for the clusters studied here, the TDSIC description improves on TDLDA deficiencies in details of the coupling to $1ph$ structures.

4 Conclusions

Our investigation of the photoabsorption spectra of two small sodium clusters with three different methods shed new light on the theoretical methods as well as on the understanding of the experiments. The local current approximation is based on a "collective" picture of excitations. It exploits information that is contained in the curvature of the ground-state energy functional, and its success in the cases studied here demonstrates that the functional, indeed, contains relevant information on the excited states. Furthermore, LCA's quantitatively accurate description of the strong excitations and partial success in describing higher lying ones shows that the concept of "collectivity" and the detailed view in terms of particle-hole excitations have more in common than expected, even for these small clusters. TDLDA has the advantage of being robust throughout a wide range of energies. It leads to a reliable description of overall features of photoabsorption spectra. The comparison with TDSIC showed, however, that details of the excitation spectrum can be rather sensitive to self-interaction effects, even for a simple metal like sodium. Thus, treating exchange and correlation on a level beyond LDA is very desirable.

The success of density-functional methods to accurately describe the excitation spectra of small clusters in general, and the LCA in particular, leads to an alternative interpretation of the photoabsorption data. Our results show that the traditional way of thinking of excitations in small metal clusters as transitions between distinct molecular states coincides nicely with the more intuitive way of understanding them as collective electronic eigenmodes, i.e., oscillations of the valence electron density. Of course, these oscillations are neither exactly like the Mie plasmon in a classical metal sphere nor like the compressional bulk plasmon. Their frequencies and oscillation patterns are determined by the clusters' intrinsic structure, which for small systems like the ones studied here must of course be described quantum mechanically. But if this is taken into account, the picture of density oscillations is well compatible with the "molecular states" point of view, and with experimental data.

Acknowledgements S.K. acknowledges discussions with M. Brack and financial support from the Deutsche Forschungsgemeinschaft under an Emmy-Noether grant.

References

1. C. R. C. Wang, S. Pollack, D. Cameron, and M. M. Kappes, Chem. Phys. Lett. **166**, 26 (1990); J. Chem. Phys. **93**, 3787 (1990).
2. K. Selby, V. Kresin, J. Masui, M. Vollmer, W. A. de Heer, A. Scheidemann, and W. D. Knight, Phys. Rev. B **43**, 4565 (1991).
3. For a recent example, see e.g. T. Doppner, S. Teuber, M. Schumacher, J. Tiggesbaumker, K.H. Meiwes-Broer, Appl. Phys. B **71**, 357 (2000).
4. C. Ellert, M. Schmidt, C. Schmitt, T. Reiners, and H. Haberland, Phys. Rev. Lett. **75**, 1731 (1995); M. Schmidt and H. Haberland, Eur. Phys. J. D **6**, 109 (1999).
5. W. Ekardt, Phys. Rev. B **31**, 6360 (1985); W. Ekardt and Z. Penzar, Phys. Rev. B **43**, 1322 (1991).
6. M. Brack, Phys. Rev. B **39**, 3533 (1989).
7. P.-G. Reinhard, M. Brack and O. Genzken, Phys. Rev. A **41**, 5568 (1990).
8. M. Madjet, C. Guet, and W. R. Johnson, Phys. Rev. A **51**, 1327 (1995).
9. U. Saalmann and R. Schmidt, Z. Phys. D **38**, 153 (1996).
10. A. Rubio, J. A. Alonso, X. Blase, L. C. Balbás, and S. G. Louie, Phys. Rev. Lett. **77**, 247 (1996); M.A.L. Marques, A. Castro, and A. Rubio, J. Chem. Phys. **115**, 3006 (2001).
11. V. Bonačic-Koutecký, J. Pittner, C. Fuchs, P. Fantucci, M. F. Guest, and J. Koutecký, J. Chem. Phys. **104**, 1427 (1996).
12. C. A. Ullrich, P.-G. Reinhard, and E. Suraud, Phys. Rev. A **62**, 053202 (2000).
13. I. Vasiliev, S. Öğüt, and J. R. Chelikowsky, Phys. Rev. Lett. **82**, 1919 (1999).
14. S. Kümmel, M. Brack, and P.-G. Reinhard, Phys. Rev. B **62**, 7602 (2000).
15. S. J. A. Gisbergen, J. M. Pacheco, and E. J. Baerends, Phys. Rev. A **63** 062301 (2001).
16. For overviews see, e.g., E. K. U. Gross, C. A. Ullrich, and U. J. Gossmann, in *Density Functional Theory*, edited by E. K. U. Gross and R. M. Dreizler (NATO ASI series, Plenum, New York 1994); E. K. U. Gross, J. F. Dobson, and M. Petersilka, in *Density Functional Theory*, edited by R. F. Nalewajski (Topics in Current Chemistry, Vol. 181, Springer, Berlin, 1996); for interesting recent caveats see N.T. Maitra and K. Burke, Phys. Rev. A **63**, 042501 (2001).
17. S. Kümmel and M. Brack, Phys. Rev. A **64**, 022506 (2001).
18. J. P. Perdew and Y. Wang, Phys. Rev. B **45**, 13244 (1992).
19. J. P. Perdew, K. Burke, and M. Ernzerhof, Phys. Rev. Lett. **77**, 3865 (1996).
20. S. Kümmel, J. Akola, and M. Manninen, Phys. Rev. Lett. **84**, 3827 (2000).
21. At the heart of this matter is Eq. (27) of Ref. [17].
22. F. Calvayrac, P.-G. Reinhard, E. Suraud, C. Ullrich, Phys. Rep. **337**, 493 (2000).
23. K. Yabana, G.F. Bertsch, Z. Phys. D **42**, 219 (1997).
24. F. Calvayrac, E. Suraud, P.-G. Reinhard, Ann. Phys. **254** (N.Y.), 125 (1997).
25. W. R. Fredrickson and W. W. Watson, Phys. Rev. **30**, 429 (1927); presentation of experimental data adapted from Ref. [13].
26. An extensive discussion of the sumrule approach can be found, e.g., in M. Brack, Rev. Mod. Phys. **65**, 667 (1993).
27. S. Kümmel, *Structural and Optical Properties of Sodium Clusters studied in Density Functional Theory* (Logos Verlag, Berlin, 2000) 37.
28. M. Moseler, H. Häkkinen, U. Landman, Phys. Rev. Lett. **87**, 053401 (2001).